AGRICULTURAL ENGINEERING SOLUTIONS
ISSN: 2181-399X Volume 2, Issue 6, 2024

RESEARCHING THE PARAMETERS OF THE DISC PLOUGH AND THE DIAMETER OF ITS SUPPORT DISC

R. Hamroev[1] M. Xudoyberdiyev[1]

[1]Tashkent State Technical University, university str. 2, Tashkent 100095, Uzbekistan.

Abstract. In this article it is described that the results of studies on the research of the technological working process of the disc plough and the determination of the diameter D, the radius of curvature R of its working bodies, and the transverse and longitudinal distances between them, as well as the diameter of the disc plough support. Therefore, according to the obtained expressions, the diameter and radius of curvature of the working bodies are at least 62 and 73 cm, respectively, the transverse distance between them is in the range of 32-35 cm, and the longitudinal distance is at least 53 cm, and according to the results of the research, the disc plow works without deviation to the side during the work process and in order for its coverage width to be stable, the diameter of its support disc should be between 500-550 mm.

Key words: plough, longitude, distance, rotary, tillage, soil, energy, efficient, quality, crop

Introduction. In the world, the development of energy-resource-efficient and high-performance soil tillage machines occupies a leading position. "Every year 1.6 bln. taking into account the cultivation of more than one hectare" [1], the development of high-quality and productive and energy-resource-efficient agricultural and post-harvest machines and machines is one of the important tasks [2]. At the same time, great attention is paid to the development and use of ploughs with low energy consumption.

On earth, scientific and research work is being carried out aimed at developing new scientific and technical bases of resource-saving technologies for preparing fields for planting agricultural crops and the technical means that implement them [3]. In this direction, it is important to carry out targeted scientific research on the development of forward and rotary soil tillage machines and ensuring resource efficiency during the interaction of their working parts with the soil.

In the world, comprehensive measures have been taken to reduce labour and energy consumption in agricultural production, save resources, grow agricultural crops based on advanced technologies, and develop agricultural machines with high productivity, including plowing fields with less energy and technological processes. special attention is paid to the development of technical means that ensure quality performance.

In recent years, in connection with the widespread introduction of energy-resource-efficient technologies and technical tools in agriculture, the use of disk plows, that is, the working body is in the form of a spherical disk, is gaining importance in the main tillage (ploughing) of land. Because they have less resistance to traction than reverse plows, high productivity, work without getting stuck in plant residues and weeds. It should also be noted that due to the high level of soil grinding and grinding of discs, high-quality soil preparation for planting is achieved when using disc plows [2-3].

Theoretical and experimental methods. Based on the above, studies were conducted at Tashkent State Technical University named after Islam Karimov on the development of a disk plow for the main tillage of the land in the cultivation of grain, repeated and other agricultural crops and on the basis of its parameters suitable for the soil and climate conditions of our region. This article presents the results of studies on the study of the technological work process of the disk plough and the basis of the diameter D (figure 1), the radius of curvature R and the transverse and longitudinal distances *l* between them, as well as the diameter of the base disk of the disk plough.

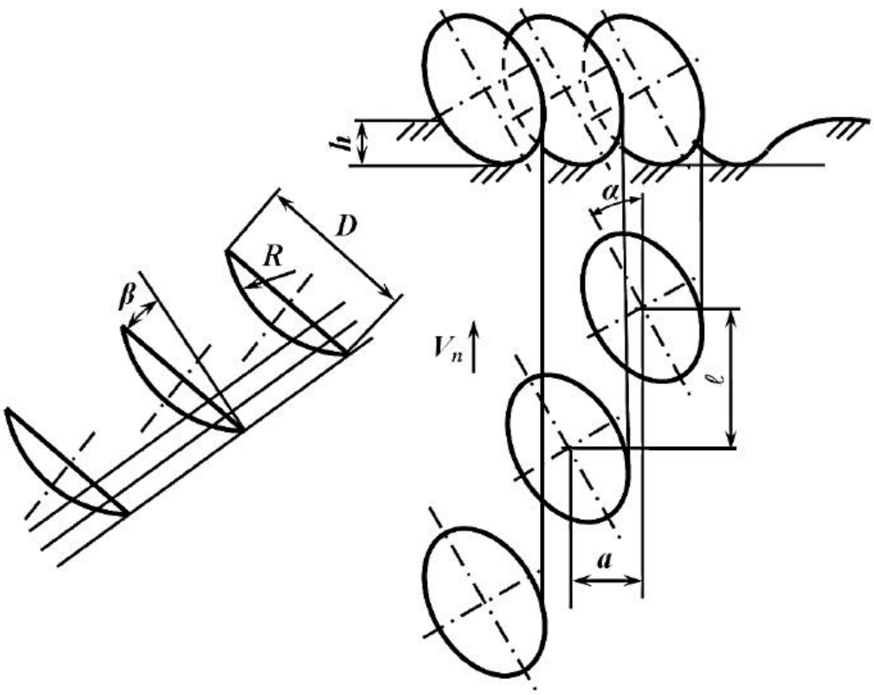

Figure 1. Workflow and parameters of disk plough

In the process of work, the discs move forward and rotate, cutting the cross-section rods from the soil (Fig. 2) and turning them sideways. As a result of this, unevenness (roundness) with a height equal to hd is formed in the bottom of the plow. Due to the deformation and pushing of the soil in the transverse direction under the influence of the working bodies, the tip parts of the irregularities formed in the bottom of the plow are damaged, and their actual height hx is always smaller than the theoretical height hd, and it, that is, the actual height of the irregularities formed in the bottom of the plow, can be determined by the following expression

$$h_x = \frac{1}{k}\left(0{,}5D - \sqrt{0{,}25D^2 - \frac{a^2}{4\sin^2\alpha}}\right)\cos\beta, \tag{1}$$

where k is the coefficient that takes into account the reduction of the height of unevenness formed at the bottom of the plow;

a, b - installation angles of working bodies relative to the direction of movement and vertical, respectively.

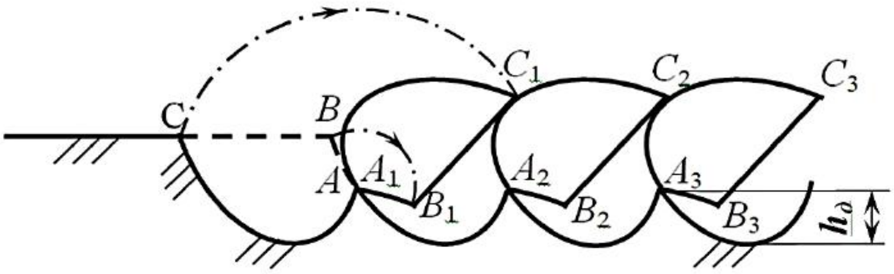

Figure 2. Cross-sectional view of the blade being sheared by the disk and the process of overturning

According to agrotechnical requirements, in order to ensure the growth and development of plants in the same conditions, the height of unevenness formed at the bottom of the plow should not exceed the permissible value, i.e. $h_x \leq 0.4$ h (where h is the depth of processing) [4-5].

In order to determine the diameter of the working body and the radius of curvature of its working surface, the following expressions were obtained from the condition that the height of the unevenness formed at the bottom of the plow does not exceed the permissible value and to ensure the even (orderly) overturning of the plows being processed

$$D \geq h\left(\frac{k_n^{\,2}\cos\beta}{1{,}6k\sin^2\alpha}+\frac{0{,}4k}{\cos\beta}\right) \tag{2}$$

and

$$R \geq \frac{h}{2\sin(\alpha_T-\alpha)}\left(\frac{k_n^2\cos\beta}{1{,}6\sin^2\alpha}+\frac{0{,}4k}{\cos\beta}\right), \tag{3}$$

where kn – is the ratio of the width of the treated plate to its thickness and

α_T - is the angle of descent of the blade from the disk.

The transverse distance between the working bodies can be determined according to the following expression, based on the condition that the plates overturned by them must occupy a steady state

$$a \geq k_n h. \tag{4}$$

To determine the longitudinal distance between the working bodies, the following expression was derived from the condition that the impact zone of the working body located behind does not reach the working body located in front

$$\ell > \sqrt{\frac{h}{\cos\beta}\left(D-\frac{h}{\cos\beta}\right)}\cos\alpha + 0{,}5\left(D-2\sqrt{\frac{h}{\cos\beta}\left(D-\frac{h}{\cos\beta}\right)}\right)\times\times\cos\beta\sin\alpha + atg\alpha. \tag{5}$$

kn=1,3; k =1,5; h=25-27sm, α =400, β=150 and α_T =650 taking quantities [5-6], according to expressions (2)-(5), the diameter and radius of curvature of the working bodies should be at least 62 and 73 cm, respectively, the transverse distance between them should be between 32-35 cm, and the longitudinal distance should be at least 53 cm was determined. In the process of work, the base disk should rest on the bottom of the bottom formed by the last body (Fig. 3), the plough should work in the horizontal plane without deviating to the side, and ensure that its actual coverage width is equal to the structural coverage width and is stable (uniform). Otherwise, the performance of the plough will deteriorate and the resistance to pulling will increase.

Theoretically, the diameter of the plough support disk can be determined by the following expression, taking into account that it is installed at an angle to the vertical

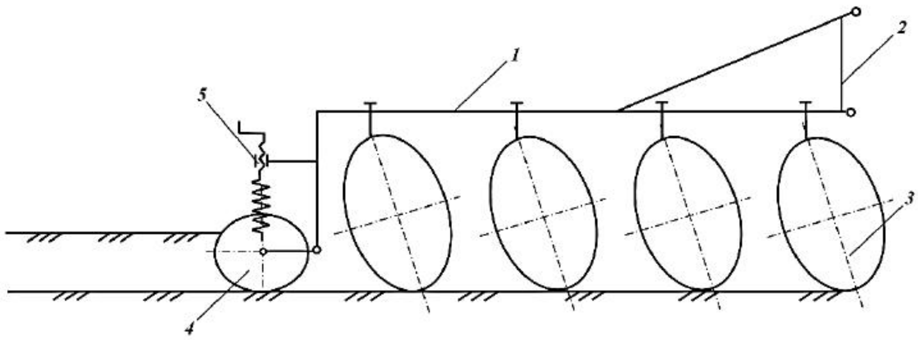

1-frame; 2-suspension machine; 3- work body; 4- base disk; 5- base disk adjustment mechanism.

Figure 3. Disk plough scheme

$$D \geq \frac{2h}{(1-\cos\alpha)\cos\beta}, \tag{6}$$

here D - diameter of the disc;

h - penetration height of the disc;

α - coverage angle with the soil;

β - installation vertical alignment.

h = 5 sm, α = 12,30 and β = 200 accepted and the calculations made according to the above expression (6) showed that the diameter of the base disk should be at least 45 cm. Special experiments were conducted to verify this obtained result. In this study, the influence of the base disk diameter change on the actual coverage width of the plough was studied. For conducting experiments, discs with diameters of 400, 450, 500 and 550 mm were prepared and they were alternately installed on a four-body plow with a constructive coverage width of 120 cm, and the change of its actual coverage width depending on the diameter of the base disc was studied.

Experiments TSt 63.02.2001 "Ispytaniya selskohozyaystvennoy tekhniki. Machines and tools for deep machining. According to Programma i metody ispytaniy», it was conducted in the field of "Sakhavatli Ibodull" farm in Yangiyol district, Tashkent region, freed from winter wheat and given moist water.

Before conducting experiments, soil moisture and hardness in 0-10, 10-20 and 20-30 cm layers were determined and their average values were 13.4, 15.2, 16.8% and 1.24, 1.73 and 2, respectively. It was equal to 64 MPa.

In conducting experiments, a disc plow was used with a TTZ 1030 tractor in its III range 1 and II range 4 transmissions.

The data obtained in the experiments are presented in Figure 4. According to their analysis, when the base discs with diameters of 400 and 450 mm are installed on the plough, the actual coverage width of the plough is 7.7 and 3.8 cm, respectively, from the design coverage width at an operating speed of 6.02 km/h and at an operating speed of 7.35 km/h. and it was bigger by 8.4 and 2.7 cm. So, when the base discs with a diameter of 400 and 450 mm were used, the plow worked sideways, that is, in the direction of the unplowed field. This can be explained by the fact that the bearing surfaces of these discs were not large enough for the plough to work without side-to-side deflection

.

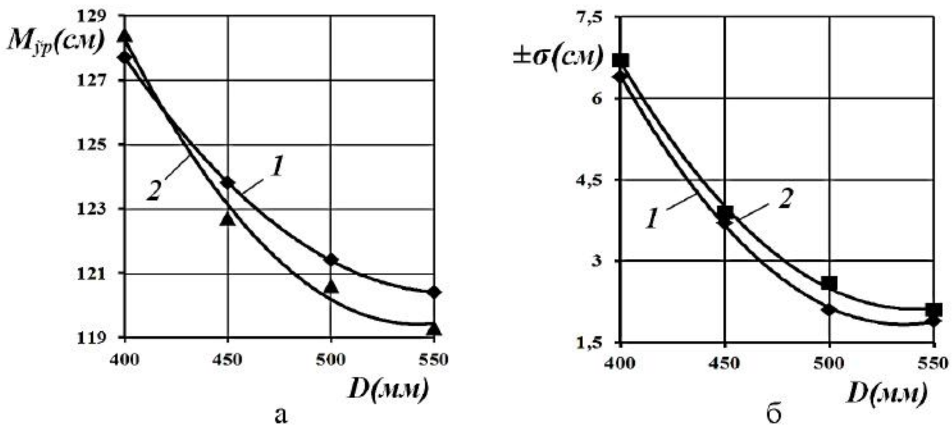

1- when the speed of movement is 6.02 km/h; 2- when the speed of movement is 7.35 km/h

Figure 4. Disc plough coverage width (a) and its root mean square deviation (b) as a function of base disc diameter

When 500 and 550 mm diameter base discs were installed on the plough, its actual coverage width was almost the same as the design coverage width, that is, the plough worked without lateral deviation.

The stability of the coverage width was improved when the diameter of the plough support disk increased from 400 mm to 500 mm, that is, its root mean square deviation decreased by ±4.3 and ±4.1 cm, respectively, at the above mentioned operating speeds. Changing the base disc diameter from 500 mm to 550 mm did not significantly affect this indicator.

Conclusion. Therefore, according to the obtained expressions, the diameter and radius of curvature of the working bodies are at least 62 and 73 cm, respectively, the transverse distance between them is in the range of 32-35 cm, and the longitudinal distance is at least 53 cm, and according to the results of the research, the disc plow works without deviation to the side during the work process and in order for its coverage width to be stable, the diameter of its support disc should be between 500-550 mm.

References.

1. Tukhtakuziev A, Ishmuradov Sh U and Abzalova M. Disc plough// Agriculture of Uzbekistan 2010 No 12 29
2. Ishmuratov Kh, Hamroev R K, Kurbonov B B and Mirzaev N N 2022 *IOP Conf. Series: Earth and Environmental Science* 2176 012096 1–6
3. Rakhmanova T T, Sultanova Sh A, Sunil Verma, Safarov J E and Dadayev G T 2021 *IOP Conf. Series: Earth and Environmental Science* 868 012080 1–6
4. Rizaev A, Malikov Z, Yuldashev A, Temirov D and Borotov A 2021 *IOP Conference Series: Materials Science and Engineering 1030* (1) 012175 // 10
5. Astanakulov K D, Karimov M R, Khudaev I, Israilova D A and Muradimova F B 2020 *IOP Conf. Series: Earth and Environmental Science* 614 012141
6. Borotov A 2020 IOP Conference Series: *Materials Science and Engineering* 883 012160.

AGRICULTURAL
ENGINEERING SOLUTIONS
ISSN: 2181-399X Volume 2, Issue 6, 2024

SUBSTANTIATIO THE PARAMETERS OF CUTTING HEIGHT IN SOYBEAN CROP HARVESTING WITH A COMBINE HARVESTER

M. Shomirzaev and A. Umirov

[1]Termez State University, 43, Street Barkamol avlod, Termez, 190111, Uzbekistan

Abstract. In this article it is observed that soybean crop elements are in the form of pods, which form from the lower part of the plant, and at high mowing heights, they may be left unharvested and loss. For this reason, it is important to correctly determine the height of harvesting soybeans. According to theoretical calculations, it was determined that when harvesting soybeans with a combine harvester, the harvesting height of the combine harvester should be set at a height of 5 cm. In experiments, when the harvesting height of the combine harvester was changed from 5 cm to 20 cm, the damage in the form of spilled pods and grain due to the effect of the motor wheel was in the range of 0.34 - 0.48 per cent, and the damage of the grain in the harvester was in the range of 1.05 - 1.23 per cent. In the experiments, unharvested pods were not observed at 5 and 10 cm mowing height, at 15 cm mowing height, such grain failure was 0.83%, and at 20 cm mowing height, it increased by 2.5 times to 2.08%. According to the results of the experiment, the productivity of the combine harvester at 5 and 10 cm harvesting height was relatively low, but the total grain loss was in the range of 1.59–1.67 per cent and did not exceed 2 per cent specified in the requirements.

Key words: soybean, crop, cutting, height, combine, harvester, grain, separator, grain damage

Introduction. Soybean is a valuable annual leguminous plant, the protein content of its grain is 40-50 per cent, and the oil content is 23-25 per cent. About 300 different food products and technical raw materials are obtained from soybeans, and important feed for livestock, poultry and fish is prepared. For this reason, soybeans are grown on an area of more than 125 million hectares worldwide. In the world the United States, Brazil, Argentina, China and India grow more soybeans. Efforts are being made to increase soybean cultivation in Uzbekistan, but due to limited land area and the main crops being cotton and wheat, it is grown as a main crop in early spring and as a follow-up crop after wheat harvest. For this purpose, a disk plow for tillage, planting and harvesting, a seeder that accurately sows seeds has been developed, and a combine operation mode has been determined [1-3].

Along with the benefits of soybean comes its challenges. These are low prices, lack of farmers' knowledge of advanced soybean cultivation technologies, and negative effects of diseases and pests [4]. All these lead to a decrease in soybean productivity.

D.R.Johnson and D.J.Major found that soybean yield depends on the time of sowing and the level of maturity.

Along with the benefits of soybean comes its challenges. These are low prices, lack of farmers' knowledge of advanced soybean cultivation technologies, and negative effects of diseases and pests. All this leads to a decrease in soybean productivity.

D.R.Johnson and D.J.Major found that soybean yield depends on the time of sowing and the level of maturity.

Soybean harvesting time also affects the quality of its grain. Therefore, it should be harvested shortly after ripening [4].

In some places, the moisture content of soybeans is high during harvesting, and in this case, it is necessary to dry the soybeans after harvesting. Otherwise, the quality of harvested grain will decrease even during its storage [5].

At present, depending on the efficiency, harvesting of soybeans with a combine harvester and reaping with reapers and after drying, threshing with threshers at the station are used [6-7].

Since soybean is a valuable plant, its productivity is not very high and is in the range of 20-35 ts/ha. The height of the soybean plant is on average 60-110 cm, depending on the varieties and cultivation techniques. Its grain is located in pods along the entire height of the stem. Therefore, cutting height is one of the most important parameters when harvesting soybeans. Because according to the biological characteristics of soybeans, the crop elements are formed from the lower part of the plant, and at a high cutting height, they remain unmowed and lead to failure. On the other hand, at a low harvesting height, the harvester complicates their work process due to the large penetration of stem mass into the threshing apparatus and grain separation parts. For this reason, it is important to correctly determine the height of harvesting soybeans. Otherwise, part of the pods will remain unharvested, causing a small harvest.

Materials and methods. In the theoretical determination of harvesting height for harvesting soybeans with a combine harvester, the height of soybean pods on the stem, the type of harvesting equipment according to the harvesting height, the movement of the segment-finger harvesting equipment and the longitudinal and transverse bending of the stems during this movement were taken into account.

In experimental studies, the effect of changing the height of the combine harvester for harvesting soybeans on the performance quality indicators of the combine was determined. Experimental studies were conducted on the Dominator-130 combine harvester in the fields of "Agrobioholding" LLC, Yangiyol district, Tashkent region. The experiments were conducted on the soybean variety "Oyjamol".

The experiments were conducted in a one-factor manner due to the extreme intensity of the harvest season and the complexity of the combine operation, as well as the impossibility of providing the same agrophone in each section of the field. Based on this, we studied the harvesting height of the grain harvester in the range from 5 cm to 20 cm, and its effect on the yield of the harvester, grain damage in the harvester and thresher was studied.

The indicators of the work quality of the harvester were grain failure in the combine harvester, grain failure in the combine harvester and unharvested pods.

Results and Discussions. When cutting soybean, the mowers must provide a "clean" cut without grinding, tearing, pulling or sliding the stems. The "Dominator-130" combine harvester is equipped with segment-finger cutting machine designed for high cutting of crops.

In this type of cutting machines, the pitch of the fingers (the distance between the axes of the fingers) $t_б$, the pitch of the segments (the distance between the axes of the segments) ts and the path of the blade Ss are equal to each other (figure 1), i.e.

$$t_b = t_c = S_c. \tag{1}$$

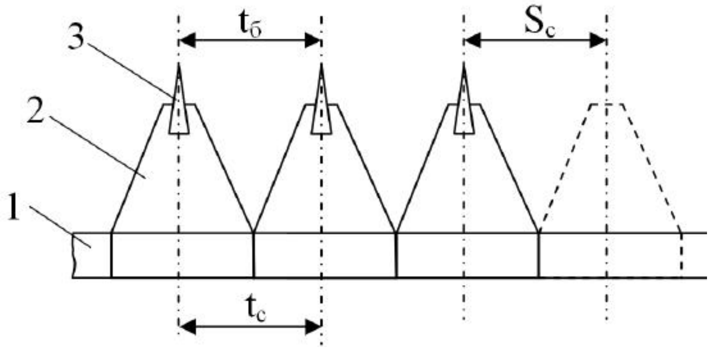

1-rail, 2-segment, 3-finger.

Figure 1. Parameters of segment-finger cutting machine

High mowers work best at a cutting height of 15-20 cm. However, it was found out from the research that 5-10% of the total pods in the soybean plant are located in the lower part of the stem, that is, up to 15 cm above the ground [8]. Therefore, it is necessary to use the mower designed for high cutting in low cutting mode. In this case, the height of the mower is reduced to a minimum position and it is ensured that it works without touching the ground.

When the harvester moves forward at a certain speed V_k, the reaper tries to bend the stalks forward. In this case, the maximum longitudinal tilt should not exceed the specified cutting height, otherwise the mower will mow the stem high.

The maximum longitudinal bending of stems during cutting is determined as follows

$$l_{\max}^{b} = y_B - y_A \,. \tag{3}$$

To determine the y_A and y_B in this expression, we write the equation of motion of the segment. According to the scheme in Figure 3.3, y_A and y_B can be determined as follows

$$y_A = \frac{V_c}{\omega} \arccos\left(\frac{b_c + S_c - b_b}{S_c}\right). \tag{3.7}$$

and

$$y_B = \frac{V_k}{\omega}\left[2\pi - \arccos\left(\frac{S_c - b_b - t_c}{S_c}\right)\right] - h'. \tag{3.9}$$

where the width of the tip of the b_c-segment, m; V_k - harvester speed, m/s; h' – the height of the segment blade, m.

Then $l_{\max}^{b}$ according to the values of y_A and y_B

$$l_{\max}^{b} = \frac{V_c}{\omega}\left(\arccos\frac{b_c + S_c - b_b}{S_c} + \arccos\frac{S_c - b_b - t_c}{S_c} - 2\pi\right) - h' \tag{3.10}$$

According to this expression, the longitudinal bending mainly depends on the ratio between the speed of the combine and the angular speed of the curve of the harvester.

Depending on the location of the pods, the cutting height can be determined as follows

$$H_{\min} \le H_{cut} \le H_{b.\min}\,, \tag{2}$$

where H_{min} - the minimum distance of the mower to the ground, m;

$H_{b.min}$ - the minimum placement height of soybeans, m.

If we consider that $H_{min}=3\ cm$, $H_{b.min}=8\ cm$, it turns out that the cutting height should be set at a height of H_{cut} = 5 cm.

Experimental studies were also conducted to verify the theoretical findings. In the experiments, the combine harvesting height was studied by changing it from 5 cm to 20 cm. When the harvesting height of the combine harvester increased from 5 cm to 20 cm, its productivity increased from 1.01 ha/h to 1.37 ha/h, i.e. 1.3 times (Table 1). This situation is explained by the fact that although the speed of the harvester is set at 1 m/s, the speed of the harvester occasionally decreased due to caution at the low cutting height, and in some cases it stopped, and it moved freely at the high cutting height.

Table 1. The influence of the change in the height of the harvester on the work quality indicators

Work quality indicators		The height of cutting the soybean, cm			
		5	10	15	20
Productivity, ha/h		1.01	1.12	1.26	1.37
Grain loss, %	in the combine header	0.34	0.45	0.48	0.44
	behind the combine	1.23	1.14	1.08	1.05
	unharvested beans	-	-	0.83	2.08

When the cutting height increased from 5 cm to 10 cm, the loss of grain in the form of beans and grains spilled by the motor wheel on the combine harvester increased from 0.34 to 0.45 per cent, while the loss of grain in the next 10 cm, 15 cm, and 20 cm of the cutting height was mortality was in the range of 0.44–0.48 per cent and remained almost unchanged.

During this range of changes in cutting height, grain failure in the combine thresher decreased from 1.23 per cent to 1.05 per cent, or 1.2 times. This situation is explained by the fact that the load of the threshing-separating working parts decreases due to the decrease in the mass of grain and stalks coming to the combine threshing machine with the increase in the height of cutting. But it was found that with the increase of cutting height, grain failure in the form of unharvested pods is observed, and the higher the cutting height.

In particular, in the experiments, there was no loss of grain in the form of unharvested pods at the cutting height of 5 and 10 cm, while the loss of grain in this form was 0.83 per cent at the cutting height of 15 cm, and it increased by 2.5 times to 2.08 per cent at the cutting height of 20 cm. According to the results of the experiment, the productivity of the combine harvester at 5 and 10 cm harvesting height was relatively low, but the total grain loss was in the range of 1.59–1.67 per cent and did not exceed 2 per cent specified in the requirements.

Conclusions. Soybean crop elements are formed from the lower part of the plant in the form of pods, and at a high cutting height, they will not be harvested, resulting in failure. Theoretical studies have shown that when harvesting soybeans with a combine harvester, the cutting height should be higher than 5 cm. In the experiments that changed the cutting height from 5 cm to 20 cm, there were no unharvested pods at 5 and 10 cm cutting height, at 15 cm cutting height, such grain failure was 0.83 per cent, and at 20 cm cutting height, it increased by 2.5 times to 2.08 per cent.

According to the results of the experiment, the productivity of the combine harvester at 5 and 10 cm harvesting height was relatively low, but the total grain loss was in the range of 1.59–1.67 per cent and did not exceed 2 per cent specified in the requirements. Therefore, when harvesting soybeans with a combine harvester, it is recommended to have a cutting height of 5-10 cm.

References.

1. Sgarbossa M, Possenti J C, Bahry C A and Modolo A J 2018 *Australian Journal of Crop Science* 12 892-897
2. Wilson R F 2004 Seed Composition in Soybeans: Improvement, Production and Uses *Madison, WI: American Society of Agronomy, Crop Science Society of America, and Soil Science Society of America* 621–628.
3. Dan Loy 1993 Soybeans for forage *Recovery-19* (Iowa: Iowa State University).
4. www.fao.org/statistics/oilseeds
5. Liu Y, Du H, Li P, Shen Y, Peng H, Liu S, and Huang X (2020) Pan-genome of wild and cultivated soybeans. Cell. 182(1): 162-176
6. Pagano MC and Miransari M 2016 The importance of soybean production worldwide *In Abiotic and biotic stresses in soybean production Academic Press* 1-26.
7. Matchanov R, Rizayev A, Astanakulov K, Tolibaev A and Karimov N 2021 Combined cotton picker with interchangeable machines *IOP Conf. Series: Earth and Environmental Science* 677 052021
8. Matchanov R, Rizaev A, Yuldashev A, Kuldoshev D and Mirzaeva M 2021 Methods for calculating the pressure loss of the air flow and energy consumed by the fan of the cotton harvester *E3S Web of Conferences* 264 04011

AGRICULTURAL ENGINEERING SOLUTIONS
ISSN: 2181-399X Volume 2, Issue 6, 2024

CREATING OF A SMALL SIZED GRAIN GRINDER MACHINE FOR SMALL LIVESTOCK, POULTRY AND FISH FARMS

F. Karshiev[1], Sh. Tursunovand D. Khudaynazarov[2]

[1]Termez State University, 43, Street Barkamol avlod, Termez, 190111, Uzbekistan
[2]Tashkent State Technical University, Tashkent, Uzbekistan

Abstract. In this article, it is presented that livestock breeding in Uzbekistan is established mainly in small farms, and more than 80 percent of the total product is produced in them. With the development of animal husbandry in small farms, there is a demand for equipment used in the preparation of feed, including the preparation of concentrated feed by grinding grains. Taking this into account, a small-sized grain grinder machine for grinding grains was developed for small farms. The height of the machine is 1170 mm, the length is 500 mm and the width is 700 mm, the weight is 45 kg, and the power of the electric motor is 1 kW. This shows that its construction is compact, metal consumption is low and energy efficient, and its use in small farms is effective enough.

Key words: small farm, small sized, grinder, grinding, grain, fodder, livestock, poultry

Introduction. In Uzbekistan, livestock, poultry and fisheries are mainly established in small farms, and they produce more than 80 percent of the total product [1-3]. In addition, households living in rural areas raise chickens, turkeys, ducks, quails and other poultry and fish, and self-sufficiency in meat and eggs is being realized. It plays an important role in food security. Along with the introduction of livestock, poultry and fish farming in small farms, their demand for feed is also increasing [2-4].

Currently, the main types of fodder used for feeding livestock are blue, coarse and grain fodder. While alfalfa and corn chopped from the field are used as green fodder, wheat, mallow, soybean straw, alfalfa hay, and corn stalks are used as coarse fodder. Wheat, barley and corn and soybeans are mainly used as grain feeds [5]. Extensive work is being done to improve the technologies and technical means to increase the yield of wheat, barley, corn, soybeans and other crops used as livestock feed, and to create new types of them [6].

With the development of animal husbandry and poultry farming in small farms, there is a demand for equipment used in feed preparation, including grain grinding. With this in mind, we have conducted research on the development of a grain grinding machine with low energy and metal consumption, simple structure and easy to use for small farms.

Materials and methods. In order to determine the distribution of livestock in Uzbekistan, livestock farms were divided into three categories - agricultural enterprises, farms and peasant farms. The number of farms and the number of livestock in their cross-section were formed based on the data obtained from statistical sources.

In order to develop a grain grinding machine, existing grain grinding machines were analyzed. For this, the advantages and disadvantages of existing machines were determined using the SWOT analysis method. Performance, energy consumption, weight, construction complexity, ease of use, universality, safety and other indicators of existing machines were compared. When developing the optimal design of the new machine, the advantages of the existing machines determined on the basis of the SWOT analysis were taken into account to the maximum extent. The main criterion for the design of the grain grinder to be developed was that it should be light, simple, and low in energy consumption, along with the high-quality implementation of the technological process.

Results and Discussions. According to statistical data, 93.4% of the total large horned cattle in Uzbekistan are small, i.e. farmers or households, 5.4% are average, i.e. farms, 155,000 heads or about 1.2% are large farms. Of the total sheep and goats, 84.0% belong to farmers or private households, 11.8% to farms and 4.2% to large-scale farms [6]. It can be seen that 85-90 percent of livestock are raised in small farms. But they don't have the energy-efficient grain grinders used in feed preparation.

With this in mind, we have developed a schematic and 3-D view of a small grain grinder for small farms (Figure 1).

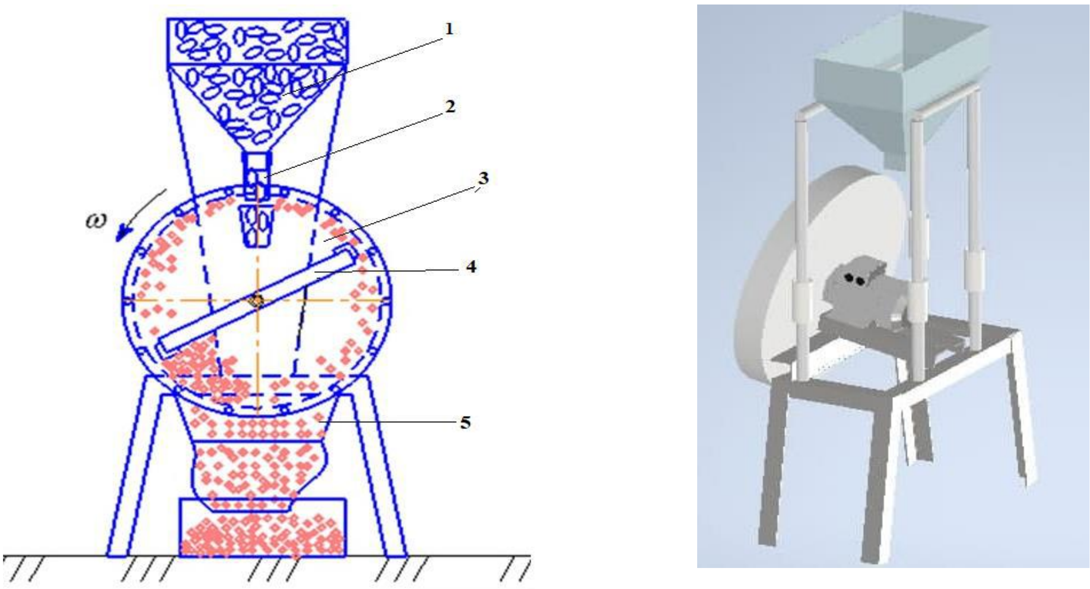

a) schematic view b) 3-D view

Figure 1. Technological and 3-D scheme of the grain grinder

The developed machine consists of a grain hopper 1, a metering chute 2, a grinding chamber 3, a hammer propeller 4, and a chute feed chute 5 (Figure 1).

During the operation of the machine, grains are placed in the hopper 1, and they are thrown into the grinding chamber 3 in a uniform manner through the standard transfer chute 2. In the grinding chamber, the grains are grinded using hammers attached to the propeller 4, and the grinded grain passes through the sieve installed at the bottom of the grinding chamber and falls into the container through the output chute 5 (Figure 1). The grain grinder is powered by an electric motor.

According to the above technological scheme and 3-D view of the grain grinder, a natural copy of it was made (Figure 2).

Figure 2. Grain grinder machine

The grain grinder machine is 1170 mm high, 500 mm long and 700 mm wide (see table).

Table. Technical description of the grain grinder

Names of indicators	The unit of measure of the indicator	The value of the indicator
Overall dimensions of the machine: - height - length - width	mm	 1170 500 700
Mass	kg	45 ± 3
Power taken from the network	kW	1

The weight of the machine was 45 kg, due to the fact that maximum attention was paid to the reduction of metal consumption and material consumption. This indicator is 1.5-2 times less than other grain grinding machines. Also, its energy consumption is not too high and it is driven by a 1 kW electric motor.

This shows that its construction is compact, metal consumption is low and energy efficient, and its use in small farms is effective enough.

Conclusions. 85-90 percent of livestock in Uzbekistan are kept in small farms. But they have difficulties in preparing grain feed because they do not have energy-efficient grain grinders used in feed preparation. Taking this into account, a grinding machine with a hammer propeller was developed for small livestock farms. The machine has a height of 1170 mm, a length of 500 mm and a width of 700 mm and is considered compact. Also, its weight is 45 kg, energy consumption is 1 kW, which indicates its low metal and energy consumption.

References.

1. Astanakulov K, Karshiev F, Gapparov Sh, Khudaynazarov D and Azizov Sh 2021 Mini grinder-shredder for farms *E3S Web of Conferences* 264 04038
2. Shomirzaev M Kh, Astanakulov K D and Babaev Kh M 2022 Research into the perforated surface of the double staged grinder-grinder *IOP Conference Series: Earth and Environmental Science* 1076 012035
3. Astanakulov K D, Kurbonov F K and Shomirzaev M Kh 2022 Development of fish feed distributor machine *IOP Conference Series: Earth and Environmental Science* 1076 012032
4. Rasulov A D, Baimakhanov K A, Eshankulov Kh M, Astanakulov K D and Kurbanov A J 2021 Important physical and mechanical properties of the mung bean seed for harvesting and cleaning process *IOP Conference Series: Earth and Environmental Science* 848 (1) 012171
5. Balabanov V I, Vitliemov P, Astanakulov K D, Ashurov N A and Khakberdiev O 2021 Biometric parameters and physical-mechanical properties of wheat and barley grown on dry lands *IOP Conference Series: Earth and Environmental Science* 868 (1) 012077
6. Baimakhanov K A, Alpamyssova G B, Astanakulov K D and Babojanov A B 2021 Development of a pneumatic drum-type seeding apparatus for two-row seeding soybean and mung bean *IOP Conference Series: Earth and Environmental Science* 839 (5) 052062
7. Tukhtakuziev A, Ishmuradov Sh U and Xudoyberdiyev M A 2021 Justification of the parameters of the disc plough *IOP Conference Series: E*

AGRICULTURAL ENGINEERING SOLUTIONS
ISSN: 2181-399X Volume 2, Issue 6, 2024

THE BASES OF METHODOLOGY OF THE THERMAL EFFECTIVENESS IN A CONVECTIVE DRYING UNIT OF THE CHAMBER TYPE

[1]O. Rakhmatov, [1]F. Rakhmatov, [1]S. Kurbanov, [1]R. Rakhmatullaev, [1]A. Kasimov[2] , N. Musayeva

[1]Gulistan State University,
[2]National research university "Tashkent Institute of Irrigation and Agricultural Mechanization Engineers", 39, Street Kari Niyazi, Tashkent, 100000, Uzbekistan

Abstract. The article deals with the issue of increasing the efficiency of the drying plant, gives theoretical prerequisites and analytical calculations and a generalized formula for determining thermal efficiency is derived. The author and the staff conducted a number of experiments on a pilot plant. According to the results of the experiments, curves of the dependence of the efficiency of the drying unit on the heating temperature of the chamber surface and at the outlet of the spent drying agent from the drying chamber were obtained. It has been proven that with an increase in the temperature of the spent drying agent, the thermal efficiency decreases. The optimum temperature of the discharge heat of the agent is considered. The expediency of using a heat-accumulating rubble nozzle was also justified, which allows to saving up to 14% of the thermal energy required for the drying process.

Key words: nutritional properties, drying, ration modes, livestock, poultry, physic-chemic

Introduction. One of the ways to conserve the nutritional properties of melons is its drying. At the same time, vitamins, trace elements and biologically active substances that are necessary for the maintenance of human life, are maximally preserved in the agricultural [1], livestock, poultry and fishers product [2]. Therefore, in terms of choosing methods and rational modes of the drying process, it is vital to be based on scientific foundations: from studying the physic-chemical properties of the product as an object of drying, selecting highly efficient and combined methods of energy supply that ensure the intensity of the process and create, as well as finding ways to save energy due to the wider use of other types of energy [3-4].

Therefore, recently all scientific directions have been focused on the creation of energy–saving drying technology using combined (by energy) solar-fuel drying plants. The authors, based on the analysis of existing drying methods and design solutions of drying plants, put forward their concept for the modernization and optimization of the drying process, as well as energy saving. The two-chamber combined solar-fuel drying plant developed by us combines the use of both solar energy and traditional - electric. The issue of providing an oscillating drying mode as an intensifying factor of this process has been solved constructively [5].

Materials and methods. The objects of research are a two-chamber convective drying plant developed and tested by the Russians for drying annular melon slices [16], which contains two parallel–located drying chambers having a rectangular cross-section, a fan, main and auxiliary electric heaters, an air distribution manifold with a V-shaped weather vane valve. Inside the chambers, curved air-guiding ailerons and eight grocery carts are installed, located on corner guides (Figure1).

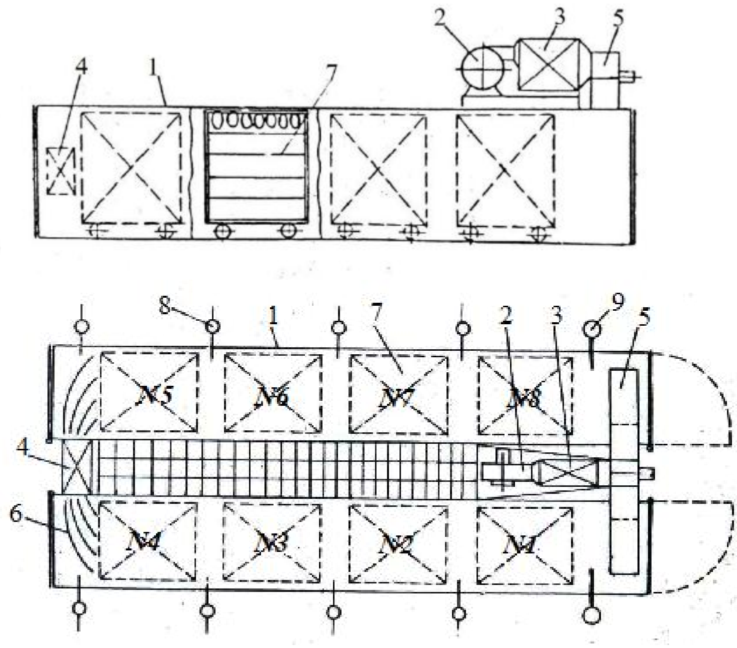

1-camera; 2-fan; 3,4-main and auxiliary electric heaters; 5-air distribution manifold; 6-ailerons; 7-grocery carts; 8-thermocouples; 9-mercury thermometer.

Figure 1. Schematic diagram of the drying plant

The grocery cart is made in the form of a spatial parallelepiped forming a rigid frame of a corner profile. On the longitudinal crossbars forming the tier, semicircular recesses are made for laying poles with melon slices, while the recesses are located on alternating crossbars with an offset of half a step. Melon slices on poles are also stacked with mixing, being placed in the volume of the cart in horizontal and vertical planes in a staggered order (Figure 2).

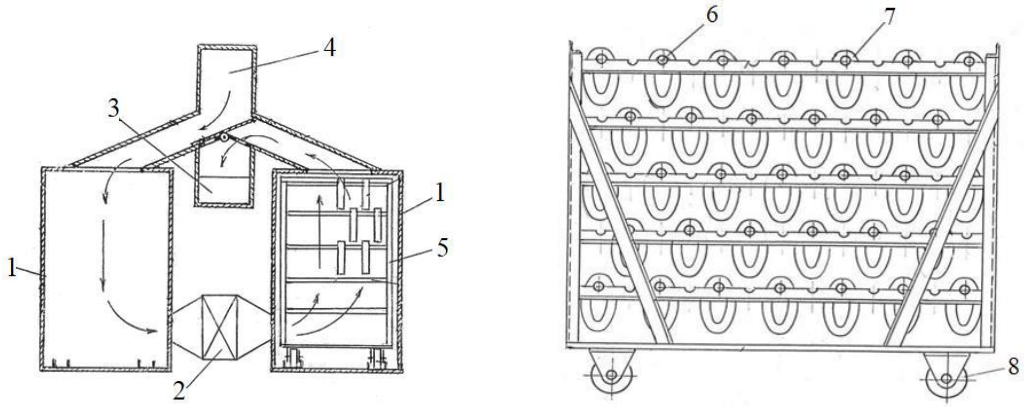

1-frame; 2-electric heater; 3-pipes; 4-air distribution manifold; 5-grocery cart; 6-wooden pole; 7-melon slice; 8-wheel.

Figure 2. Grocery cart for laying melon slices

The drying unit includes the following procedures: food carts with ring-shaped melon slices stacked on poles are loaded into both drying chambers, the doors are tightly closed and the air and heat supply system is turned on: a fan and electric heaters. At the same time, the fan pumps air through the main heater, in which it is heated to 70-80 ° C and enters one of the drying chambers through the air distribution manifold, in which it blows melon slices hung on trolleys. Due to the convective heat exchange between the hot air and the product, moisture evaporates and the air temperature drops. Then the air enters the intermediate heater, warms up to the required temperature and enters another chamber. The spent low-potential air with a temperature of 40-45 ° C is discharged through one of the sleeves of the air distribution manifold into the inter-chamber space, where poles can be suspended for pre-drying melons. By turning the V–shaped weather vane valve, the installation can be switched to an oscillating drying mode, which intensifies the dehumidification process. The oscillation period for drying melons is taken within 40-45 minutes.

Theoretical foundations and discussions. It can be observed that the regularity of the formation of the thermal efficiency of a drying plant consisting only of a solar collector (blackened chamber surface).

The thermal power supplied to the drying chamber is determined by the expression [6-7]

$$Q_{падв} = \eta_{mn}\left[\eta_{опт} q_{пад} - k_{пр}\left(\bar{t}_f - \bar{t}_o\right)\right] F_{фр}\,, \tag{1}$$

Here: η_{mn} is the efficiency coefficient of the heat receiver of the solar collector; η_{onm} is the efficiency coefficient of absorption of solar radiation by the surface of the chambers; $q_{пад}$ is the density of the incident radiation flux on the frontal surface of the chambers; k_{np} is the coefficient of total heat loss of the collector per unit of the radiation–absorbing surface; $\bar{t}_f$ – the average temperature of the coolant along the length of the chambers;

$\bar{t}_o$ –the average temperature of the coolant in the heat sink channel, ° C $F_{фр}$; – the area of the frontal radiation-absorbing surface of the chambers, m2.

On the other hand, this thermal power is equal to [7-8]

$$Q_{подв} = G_в c_в (t_1 - t_0)\,, \tag{2}$$

ere :

$G_в$ – drying agent(air) consumption,*кг*;

$c_в$ – specific heat capacity of air, К;

t_1 – air temperature heated by solar radiation,

°*C*; t_o - ambient air temperature, °*C*.

$$Q_{исп} = G_{вл} r\,, \tag{4}$$

$$Q_{mn} = \sum k_n F_c (\bar{t}_к^в - t_0^в)\,, \tag{5}$$

$$Q_{сб} = G_{воз} c_{воз} (t_к^в - t_0^в)\,, \tag{6}$$

Here: $G_{вл}$ is the amount of evaporated moisture from the product, *кг*; *r* is the latent heat of vaporization, *Дж/кг*;k_n is the coefficient of heat loss through the *i*–the wall of the chamber;

$\bar{t}_к^в$ - average air temperature along the length of the drying chamber, *К*; $t_0^в$ - ambient air temperature, *К; $G_{воз}$* is the mass air consumption, *кг*.

$$\bar{t}_f = \frac{t_1 - t_o}{\ln t_1 / t_o} \tag{7}$$

and $$f_{л}^{-в} = \frac{t_1 - t_2}{\ln t_1 / t_2}. \quad (8)$$

The values of the thermal efficiency of the solar collector-η_c and the drying chamber-η_k are determined from the well-known ratios

$$\eta_c = Q_{под\,в} : Q_{пад} \quad (9)$$

and

$$\eta_к = Q_{пол} : Q_{подв}, \quad (10)$$

Here: $Q_{пад}$ - the flow of total incident radiation to the front surface of the cameras

$$Q_{пад} = q_{пад} F_{фр}. \quad (11)$$

Defining $Q_{пол}$ from (4) and substituting the obtained into the relation (10) we get

$$\eta_k = 1 - \frac{Q_{тп} + Q_{сб}}{Q_{подв}}. \quad (12)$$

The total thermal efficiency of the drying plant is defined as the product of (9) and (10), etc.

$$\eta = \eta_c \eta_к = Q_{пол} : Q_{пад}. \quad (13)$$

Substituting the values η_c and η_k, respectively from (9) and (10) into (13) and taking into account the values $Q_{пад\,в}$, $Q_{пол}$ $Q_{пад}$, and from (2), (1), (4), (5) and (6), as well as $\bar{t}_f$ and $\bar{t}_k$ from (7) and (8), after the corresponding mathematical transformations, we obtain:

$$\eta = \eta_{тп}\left[\eta_{опт} - \frac{k_{пр}}{q_{под}}\left(\frac{t_1 - t_o}{\ln\frac{t_1}{t_o}} - t_o\right)\right]\cdot\left[1 - \frac{t_2 - t_o}{t_1 - t_o} - \frac{\sum k_i\, F_i\left(\frac{t_1 - t_2}{\ln\frac{t_1}{t_2}} - t_o\right)}{\eta_{тп}\cdot q_{пад}\cdot F_{фр}\left[\eta_{опт} - \frac{k_{пр}}{q_{пад}}\left(\frac{t_1 - t_o}{l_n\frac{t_1}{t_o}} - t_o\right)\right]}\right]. \quad (14)$$

Research results and their discussion. Figure 3 depicts the curves of the dependence of the thermal efficiency of the drying unit (η) on the heating temperature of the blackened surface of the chamber (t_1) and at the outlet of the drying chamber (t_2), which in the first approximation are close to the real operational characteristics of solar-fuel convective type installations.

As follows from the graphs of Fig.3, other things being equal, an increase in the temperature of the spent drying agent (t_2) leads to a decrease in the thermal efficiency of the dryer. So, $t_1 = 70^0 C$ with an increase t_2 from 35 ° C (during a constant drying rate) to 50 ° C in the final stage of the drying process, the decrease η is from 0.38 to 0.23, i.e. by 39.5%.

It also follows from the graphs that the dependence $\eta = f(t)$ is almost linear only at t_2 *=35 °C*. At t_2 *=45 °C*, with an increase of t_1 *= 60 °C*, the value η first rises to 0.29, and then drops. At t_2 *=50* °the maximum efficiency value η is at t_1 *= 70 °C* and corresponds to 0.24.

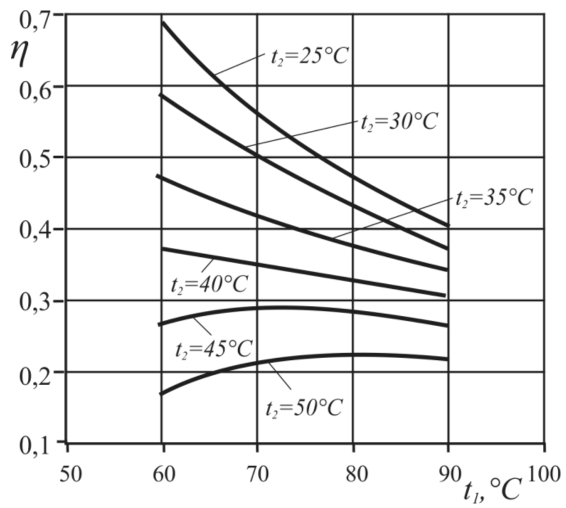

Figure 3. The dependence of the efficiency of the drying unit on the heating temperature of the chamber surface (t_1) and at the outlet of the drying chamber (t_2).

According to the based solution (14) and graphical dependencies $\eta = f(t_1, t_2)$, it is possible to optimize the temperature of the discharge drying agent. The energy-saving mode of operation of the drying unit is possible with the use of regenerative heat accumulators. In the second period of the drying process, when the temperature of the drying agent at the outlet of the chambers becomes higher than the temperature of the wet thermometer (t_m), for example by 8-10 ° C or more, the drying agent is passed through a rubble heat accumulator, which gives its heat to the nozzle and is released into the environment. At night, the sucked air passes through the rubble nozzle and is heated by accumulated energy. The temperature controller in the "on-off" mode reduces the power of the main heat source (electric heater) and thereby provides an energy-saving mode. The overall, thermal and aerodynamic characteristics of regenerative nozzle accumulators are determined depending on the performance of the drying unit, taking into account the thermo-physical properties of the nozzle, its porosity and the dimensions of the nozzle elements.

As the results of preliminary studies have shown, the heat savings during the drying of agricultural products according to the proposed scheme is 27-28%, including 14-15% from the use of solar radiation and up to 14% due to the regeneration of waste heat through nozzle batteries.

Conclusions. Due to the conducted research followings can be concluded:

1. The upgraded two-chamber combined solar-fuel drying plant combines the use of both solar energy and traditional - electric, optimizing the drying process. Such a constructive solution provides an oscillating drying mode, where the intensity of moisture extraction is achieved by 30-35%.

2. Based on the solution of graphical dependencies $\eta = f(t_1, t_2)$, it is possible to optimize the temperature of the discharge drying agent. The energy-saving mode of operation of the drying unit is possible with the use of regenerative heat accumulators.

3. It is established that the temperature controller in the "on-off" mode reduces the power of the main heat source (electric heater) and thereby provides an energy-saving mode.

4. Heat savings during the drying process according to the proposed scheme is 27-28%, including 14-15% from the use of solar radiation and up to 14% due to the regeneration of waste heat through the nozzle batteries.

References.

1. Astanakulov K D, Balabanov V I, Vitliemov P, Ashurov N A and Khakberdiev O 2021 Biometric indicators and physical-mechanical properties of wheat and barley grown on dry lands *IOP Conference Series: Earth and Environmental Science* **868 (1)** 012077
2. Astanakulov K D, Rasulov A D, Baimakhanov K A, Eshankulov Kh M and Kurbanov A J 2021 Important physical and mechanical properties of the mung bean seed for harvesting and cleaning process *IOP Conference Series: Earth and Environmental Science* **848 (1)** 012171
3. Astanakulov K D, Baimakhanov K A, Alpamyssova G B, Babojanov A B 2021 Development of a pneumatic drum-type seeding apparatus for two-row seeding soybean and mung bean *IOP Conference Series: Earth and Environmental Science* **839 (5)** 052062
4. Astanakulov K 2020 Adaptation mechanic sowing apparatus for sowing soybean seeds with less damaging *IOP Conference Series: Materials Science and Engineering* **883** 012137
5. Astanakulov K D, Umirov A T, Sultanbekova P S and Alpamyssova G B 2021 Determination of working indicators of New Holland TS-5060 combine for soy bean harvesting *IOP Conference Series: Earth and Environmental Science* **839 (5)** 052048
6. Astanakulov K 2020 Parameters and indicators of the longitudinal-transverse oscillation sieve *IOP Conference Series: Materials Science and Engineering* **883** 012151
7. Sattarov N E, Borotov A N, Yunusov R F and Yangiboev A E 2022 Growth and development of bulls of the red steppe breed in lightweight buildings *IOP Conference Series: Earth and Environmental Science* **1076** 012081
8. Borotov A N 2022 Research the parameters of cutter bar of the rotor of a green stalk forage chopper *IOP Conference Series: Earth and Environmental Science* **1076** 012027

AGRICULTURAL ENGINEERING SOLUTIONS
ISSN: 2181-399X Volume 2, Issue 6, 2024

RESEARCHING OF STATIC AND DYNAMIC PROPERTIES OF ELECTROMAGNETIC SENSOR

A. Djalilov[1*], O. Nazarov[1], S. Urolov[2], G. Esemuratova[3]

[1]National research university "Tashkent Institute of Irrigation and Agricultural Mechanization Engineers", 39, Street Kari Niyazi, Tashkent, 100000, Uzbekistan.
[2] Faculty of Electronics and Automation, Tashkent State Technical University, University str. 2, Tashkent, Uzbekistan
[3]Department of Electrical Engineering and Metrology, Karakalpak State University Named After Berdakh, Ch. Abdirov str. 1, 230115, Nukus, Uzbekistan

Abstract. In recent years, in many parts of the world, including Central Asia, water scarcity has adversely affected the region’s economy, livelihoods and interstate relations. This increases the demand for modern metering equipment for flow and water level. Currently, water management systems in developed countries use and measure water meters with different designs to measure and control the flow and level of water. For this reason, this article investigates the static and dynamic characteristics of an electromagnetic sensor used to measure water flow and level and develops its software.

Key word: static, dynamic, measure, electromagnet, sensor, automatic, gate, drainage, system

Introduction. In the early 1990s, the misuse of water resources led to serious economic, environmental and social problems in the Central Asian region, a shortage of water resources, and an increase in the level of salinity of irrigated lands. It is impossible to imagine the development of agriculture without water resources. Agriculture is the backbone of the country's economy and is an important industry [1]. Currently, the automation of the agricultural sector is one of the most important issues for all countries. The rapid growth of the world's population indicates the need for a large-scale development of equipment and technologies that can fully meet the needs for food and consumer demand [2], [3], [4]. The technology of food production requires their improvement and measurement accuracy to meet the ever-increasing needs of consumers [5]. Of great importance is the complete and high-quality provision of the population with agricultural products [6,7,8].

In this regard, scientists from the agar industry conducted scientific research on sensors with high accuracy and sensitivity in calculating and controlling the amount of water consumed in order to effectively use water resources [9].

The President of the Republic of Uzbekistan in the strategy of action in five priority areas of development of the country further improve the reclamation of irrigated lands, develop a network of reclamation and irrigation facilities, introduce intensive methods into the agricultural production, primarily modern agricultural technologies, save water and resources, use agricultural equipment with high productivity emphasized the need to carry out work on this issue as soon as possible.

At the moment, the Department of Electrical Engineering and Mechatronics is conducting scientific research on the development and creation of a new class of sensors for irrigation and drainage systems [10,11]. These sensors have high and constant sensitivity, accuracy and reliability at all points of the measuring range for automatic measurement of water flow.

Methods. The basis of the circuit of the developed electromagnetic sensor is an inductive sensor with a movable screen formed by a traditional П-shaped magnetic circuit [12].

The following basic requirements are imposed on the sensors of the automatic gate control system:

1. The static characteristics of the sensors must be linear U=f(x).

2. Metrological and dynamic characteristics of irrigation and drainage systems must comply with the operating conditions.

3. In position 0 of the moving screen, the output signal of the sensors, that is, the residual EMF, should be minimal.

A biparametric electromagnetic sensor operating in a resonant mode largely satisfies the above requirements [10,11].

The use of a liquid crystal capacitor in the existing design, the technological complexity of manufacturing capacitors of variable resistance, the uneven distribution of magnetic induction along the magnetic circuit increase the degree of non-linearity of the static characteristic of the displacement sensor ($\varepsilon \geq 1{,}0 \div 2{,}0\%$) and reduce the measurement accuracy.

The development of the idea of adaptation in the theory of automatic tuning, in particular self-adjusting and parametrically controlled systems, solves such issues as improving the metrological and dynamic characteristics of sensors over the entire measurement range, ensuring the optimal measurement process.

Results and Discussion. In the article, a linear displacement sensor was studied, in which the adjustment to the resonance mode was worked out by creating an additional circuit with parametric feedback.

The functional diagram of the developed electromagnetic sensor is shown in Figure 1.

It consists of a П-shaped permanent magnetic circuit, on its basis the primary excitation coil W_1 and the measuring coil W_2 are placed. And the input signal of the sensor is a movable armature - the shift of the screen along the X coordinate. A series of windings with a constant capacitance C and an inductance equal to L_2, through an additional resistor $R_{add} = \sqrt{R^2{}_2 + (\omega L)^2} \big/ 15 \div 20$, the value of which is slightly larger than the output end of the coil W_2, forms the resonant circuit of the coil W_2.

It is desirable to provide a resonance mode, i.e. φ_u-φ_i=0 (φ_U and φ_i are the shift angle between the output voltage U_{out} and the current obtained from the secondary circuit W_2) over the entire measurement range using a phase-sensitive detector (PSD), Uout is fed to the signal input through a square-phase torsion (SPT), and the voltage drop across the resistance R_{add} is transmitted to its basic input.

With such a connection, a signal proportional to the phase difference and the sign of $\Delta\varphi = \varphi_u - \varphi_i$ is formed at the output of the phase-sensitive detector (PSD). This signal is used to automatically control the variable a measuring frequency generator (MFG) in frequency. And the excitation coil of the electromagnetic sensor W_1 is provided as a DC source.

Thus, the proposed sensor is a closed system of extreme adjustment, adapted to the maximum sensitivity, which is achieved by maintaining the resonance mode.

Realization of the resonance regime in all ranges increases the metrological and dynamic properties of the electromagnetic sensor.

1. Creation of maximum sensitivity with automatic tuning to the resonance mode, regardless of temperature and time instability;

2. The presence of a stable connection with parasitic conduction;

3. It is possible to adjust the output signal in any range by changing the number of windings.

4. It is possible to choose the sensor material and the geometric dimensions of the magnetic circuit;

5. It is possible to reduce the size of the sensor and achieve greater stability.

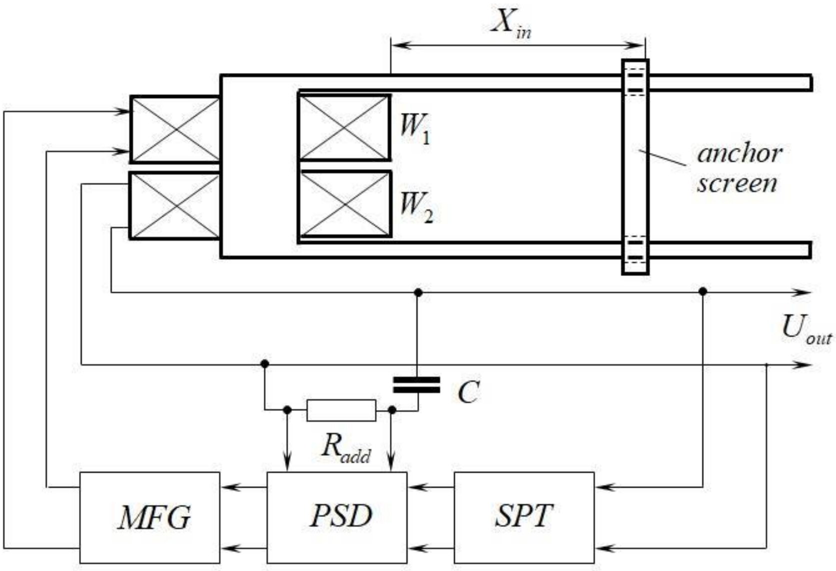

Figure 1. Functional scheme of an electromagnetic sensor with a Π-shaped magnetic conductor.

All of these properties increase the measurement accuracy of the sensor.

The static characteristic of the electromagnetic sensor analyzed by us was obtained from the circuit shown in Figure 3.

The inductance of the secondary winding is related to the movement of the armature-screen as follows:

$$L_2 = W^2{}_2 \mu_0 \frac{b \cdot x}{\delta} \tag{1}$$

where *b* and δ are the width of the magnetic circuit and the distance between the rods.

If the output voltage of the measuring frequency generator (MFG) is denoted by U_{FG}, then the voltage obtained from the secondary winding, excluding the magnetic flux in the air, will be as follows:

$$U_{out} = \frac{\omega L_2 U_{MFG}(W_1/W_2)}{\sqrt{(R_{add}+R_{W_2})^2 + (\omega L_2 - 1/\omega C_2)^2}} \tag{2}$$

where $\omega = 2\pi f$ is the angular frequency of the measuring frequency generator.

Taking into account the fact that in the resonant mode $\varphi_u - \varphi_i = 0$, or $\omega L_2 - 1/\omega C_2 = 0$ (3), expression (2) is fulfilled as follows:

$$U_{out} = \frac{\omega L_2 U_{MFG}(W_1/W_2)}{R_{add}+R_{W_2}} \tag{4}$$

If we compare expressions (2) and (4), then it increases to the maximum value of sensitivity, that is, to a state equal to the originality of the resonance circuit.

To calculate the static characteristics of an electromagnetic sensor, a program was developed in the DELPHI 7.0 programming language, which runs on any version of the WINDOWS operating system. The general interface of the developed program is shown in Figure 2.

On fig. 3 is a block diagram of the developed electromagnetic sensor. The structural diagram of the sensor allows not only the interaction of the internal physical or mathematical parameters of the sensor, but also the connection between each of its elements or use in control systems.

As a result of the analysis of the functional diagram of the sensor presented in fig. 1, and its block diagram (Figure 3), we will compose a system of equations using real parameters. This system of equations takes into account the effect of changing the frequency ω on the system, the time constant and the gains of the phase-sensitive detector (PSD), frequency generator (MFG) and a square-phase torsion (SPT).

From the analysis of the principle of operation of the sensor and (1) formulas, some features of the block diagram, that is, the presence of an additive voltage channel, and a parametric channel in frequency, and (1) a nonlinear link written by the expression, a square-phase torsion (SPT), a phase-sensitive detector (PSD) consists of a common linear path and an amplifier and a measuring frequency generator (MFG), each of which forms a dynamic link.

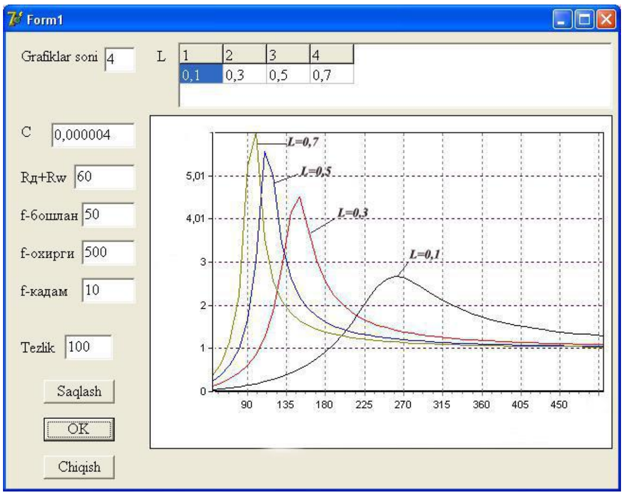

Figure 2. Static characteristic of the electromagnetic sensor.

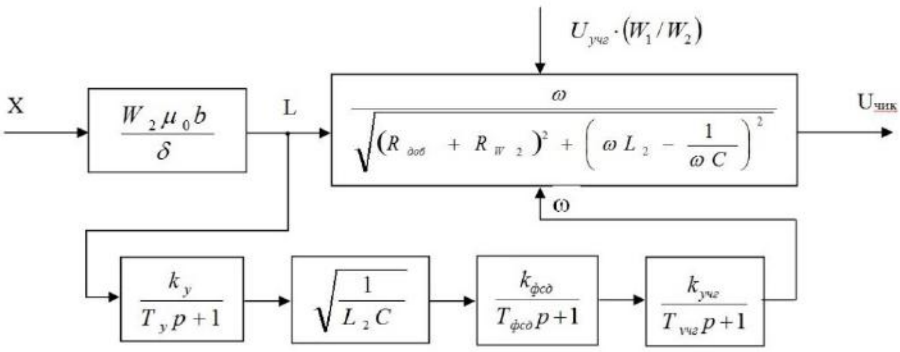

Figure 3. Structural diagram of an electromagnetic sensor.

According to the block diagram (Figure 3), for the linear part, we can write the following:

$$(T_{SPT}\,p+1)(T_{PSD}\,p+1)(T_g\,p+1)\cdot W_2^2\mu_0\frac{b}{\delta}\cdot x = k_{SPT}\cdot k_{PSD}\cdot k_{MFG}\cdot k_y\cdot U_{out} \qquad (5)$$

We combine the system of equations (2), (3) and (4) and bring it to a form convenient for numerical solution by the Runge-Kutta method:

$$\left.\begin{aligned}
&L=\frac{W_2^2\mu_0 b}{\delta}\cdot x\,;\\
&\frac{dy_1}{dt}+\frac{1}{T_y}y_1=\frac{1}{T_y}k_y L\,;\\
&y_2=\sqrt{\frac{1}{y_1 C}}\,;\\
&\frac{dy_3}{dt}+\frac{1}{T_{PSD}}\cdot y_3=\frac{1}{T_{PSD}}\cdot k_{PSD}\cdot y_2\,;\\
&\frac{dU}{dt}+\frac{1}{T_{MFG}}\cdot\omega=\frac{1}{T_{MFG}}\cdot k_{MFG}\cdot y_3\,;\\
&U_{out}=\frac{LU_{MFG}\cdot W_1/W_2}{\sqrt{\left(R_{add}+R_{W_2}\right)^2+\left(\omega L-\dfrac{1}{\omega C}\right)^2}}\,;
\end{aligned}\right\}\qquad(6)$$

Equations for the static and dynamic characteristics of the sensor can be made taking into account the limits of parameter change in formula (6). To solve formula (6), a special program was developed in the DELPHI 7.0 language.

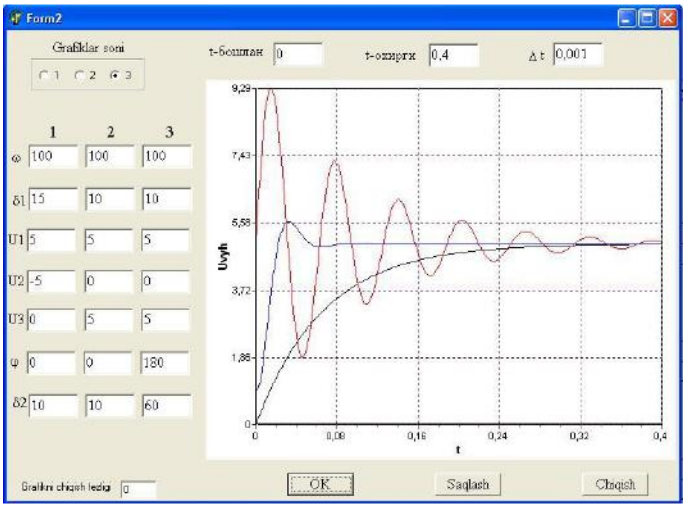

Figure 4. Dynamic characteristics of the electromagnetic sensor.

Using this program, you can calculate a family of characteristics of transient processes with a single stepwise change in displacement X (Figure 4). You can create various characteristics by changing the coefficients and capacitance of the capacitor based on the built-in program.

$$T_{PSD}=0{,}01;T_{SPT}=0{,}002-0{,}02;T_{\Gamma}=0{,}0005\div0{,}005s;k_{PSD}=0{,}15;k_y=5{,}0-20{,}0.$$

$$k_{PSD}=0{,}1;k_{\Gamma}=10-20{,}0;W_1/W_2=1;U_{MFG}=1V;C=1\,m\text{kF};L=0{,}1-0{,}7.$$

It can be seen from the expressions that when the condition of expression (2) is met, the first equation of system (6) becomes linear, while the gain increases and maximum sensitivity is provided.

As can be seen from expression (6), $0 \le \frac{U_{чик}(x)}{x} \le k$, in the chain of the main channel of the system satisfies the condition $x \ne U(0) = 0$ and has the following properties: $U_{out(p)}$ is a continuous function; $pU(p) > 0$ where $p \ne 0$ $U_{out}(0) = 0$;

$$\int_{0}^{\pm\infty} U_{out}(0)dp = \infty, \quad (7)$$

where $U_{out(0)}$ – $U_{out}(x,C,R_{W2},,W_1,W_2)$ is a short designation of the function, which is a static characteristic of the sensor.

x,C,R_{W2},W_1,W_2 are usually the current options.

Theoretical and experimental studies show that for the limits of parameter change, for the stationary state of the linear part of the system, one can choose such a real number *h* that in all cases $\omega>0$ the known absolute state of stability of V. M. Popov is equally satisfied, that is:

$$R_e\left[(1+j\omega h)W_l(j\omega)\right]+1/k>1, \quad (8)$$

where $W_l(j\omega)$ is the amplitude phase-frequency characteristic of the linear section, *k* is the slope of the straight line limiting the nonlinearity from above.

Conclusions. Thus, checking this class of sensors for absolute stability by the method of V. M. Popov shows that it belongs to an automatic excitation system with parametric coupling and has a dynamic characteristic of a linear excitation system.

In improving the accuracy and sensitivity of the developed electromagnetic sensor, its adjustment to the resonant mode is of great importance. With the help of a program developed in the DELPHI 7.0 programming language, which runs on any version of the WINDOWS operating system, we can set the sensor for resonance mode by quickly and easily changing the necessary parameters.

References.

1. Khaled Obaideen, Bashria A A Yousef, Maryam Nooman AlMallahi 2022 An overview of smart irrigation systems using IoT. *Energy Nexus*. Volume 7 September 100124
2. Liakos K G, Busato P Moshou, D, Pearson S and Bochtis D 2018 Machine learning in agriculture a review *Sensors* 18 (8) p 2674
3. Jha K, Doshi A, Patel P, and Shah M 2019 A comprehensive review on automation in agriculture using artificial intelligence *Artif. Intell Agric* 2 pp 1-12
4. Khan N, Ray R L, Sargani G R, Ihtisham M, Khayyam M and Ismail S 2021 Current progress and future prospects of agriculture technology: gateway to sustainable agriculture. *Sustainability*, 13 (9) p 4883
5. Nasiakou A, Vavalis M and Zimeris D 2016 Smart energy for smart irrigation *Comput. Electron. Agric* 129 pp 74-83
6. Ojha T, Misra S and Raghuwanshi N S 2015 Wireless sensor networks for agriculture: the state-of-the-art in practice and future challenges *Comput. Electron. Agric* 118 pp 66-84
7. Weersink A, Fraser E, Pannell D, Duncan E and Rotz S 2018 Opportunities and challenges for big data in agricultural and environmental analysis *Annu Rev Resour Econ*, 10 (1) pp 19-37
8. Alcamo J 2019 Water quality and its interlinkages with the sustainable development goals. *Curr Opin Environ Sustain* 36 pp 126-140
9. Djalilov A, Juraeva N, Nazarov O and Urolov S 2020 *IOP Conf Ser Earth Environ Sci* **614**

012044
10. Baratov R J 2004 New measuring sensors for irrigation *Mechanization and electrification of agriculture*. No7 pp 11-12
11. Yakubov M S, Baratov R J, Shoyimov Y Y and Djalilov A U 2007 Some issues of statics and dynamics of inductive linear displacement transducers with maximum sensitivity *Journal of Informatics and energy problems* Tashkent TIIAME pp 36-45
12. Frayden Dj 2006 *Modern sensors* Moscow Texnosfera p 592